ISSN 0036-0244, Russian Journal of Physical Chemistry A, 2016, Vol. 90, No. 1, pp. 25–30. © Pleiades Publishing, Ltd., 2016.
Original Russian Text © P.O. Andreev, E.I. Sal'nikova, O.V. Andreev, I.M. Kovenskii, 2016, published in Zhurnal Fizicheskoi Khimii, 2016, Vol. 90, No. 1, pp. 16–21.

CHEMICAL KINETICS AND CATALYSIS

Kinetic Schemes of Chemical Transformations and Particle Morphology upon Interaction between $Ln_2(SO_4)_3$ (Ln = La, Pr, Nd, Sm) and Hydrogen

P. O. Andreev[a], E. I. Sal'nikova[b, c], O. V. Andreev[c], and I. M. Kovenskii[a]

[a] *Tyumen State Oil and Gas University, Tyumen, 625000 Russia*
[b] *Agrarian State University of Northern Zauralye, Tyumen, 625003 Russia*
[c] *Tyumen State University, Tyumen, 625003 Russia*
e-mail: elenasalnikova213@gmail.com

Received January 14, 2015

Abstract—The phase compositions of samples obtained during the treatment of anhydrous sulfates $Ln_2(SO_4)_3$ (Ln = La, Pr, Nd, Sm) in a stream with an excess of hydrogen in the temperature range of 400 to 1100°C at exposures of up to 420 min are determined. Kinetic schemes are compiled for the chemical transformations and changes of phase composition of the mixtures in coordinates of temperature and time that have six fields of the phase combinations: $Ln_2(SO_4)_3$, $Ln_2(SO_4)_3 + Ln_2O_2SO_4$, $Ln_2O_2SO_4$, $Ln_2O_2SO_4 + Ln_2O_2S$, Ln_2O_2S, and $Ln_2O_2S + Ln_2O_3$. Single-phase samples of $Ln_2O_2SO_4$ compounds are obtained at temperatures (°C) of 540–560 (La), 460–520 (Pr), 470–520 (Nd), and 480–520 (Sm). The temperatures (°C) of Ln_2O_2S compounds are 580–920 (La), 600–900 (Pr), 600–900 (Nd), and 600–800 (Sm). It is shown via electron microscopy that particles of $La_2(SO_4)_3$ in the shape of cylinders are converted into flakes of $Ln_2O_2SO_4$, predominantly flat Ln_2O_2S crystallites.

Keywords: sulfates, oxysulfides of rare-earth elements, the kinetic scheme of chemical reactions, particle morphology.

DOI: 10.1134/S0036024416010027

INTRODUCTION

Oxysulfides of rare earth elements (REE) Ln_2O_2S (Ln = La–Lu) and yttrium are studied as luminophores, laser and optical materials [1–11]. Polycrystalline oxysulfides or solid solutions based on them, doped with Nd^{3+}, Er^{3+}, Tm^{3+}, or Yb^{3+} ions, are highly effective anti-Stokes luminophores of green and blue glow, and are used for the manufacture of LEDs and display boards [1–4]. The solid solution of $Gd_2O_2S:Eu^{3+}$ is a promising new biomarker tool [5].

The method for preparing Ln_2O_2S compounds, which includes treating REE sulfates in a flow of hydrogen, is technological. It does not contaminate the material, and the product is manufactured in one step without the use of additional reagents [2, 6–10]. The development of the process technology is based on data on the phase composition of the mixture, depending on the temperature and the processing time—kinetic schemes that are widely used in metallurgical science [6–8]. A kinetic diagram for the flow of system $Ln_2O_2SO_4$–H_2 (Ln = La, Pr, Nd, Sm) was built in [6]. It had five fields of different combinations of phases: $Ln_2(SO_4)_3$; $Ln_2(SO_4)_3 + Ln_2O_2SO_4$; $Ln_2O_2SO_4$; $Ln_2O_2SO_4 + Ln_2O_2S$; Ln_2O_2S; $Ln_2O_2S + Ln_2O_3$. The temperatures of reaction product formation,

$$Ln_2O_2SO_4 + 4H_2 = Ln_2O_2S + 4H_2O,$$

$$Ln_2O_2SO_4 + H_2 = Ln_2O_3 + SO_2 + H_2O$$

were found to be 610–630 and 820–950°C, respectively. The temperature intervals of homogeneous Ln_2O_2S phase formation naturally shrank: 490–950°C (La); 630–950°C (Pr); 630–910°C (Nd); 630–820°C (Sm) [6–10].

Kinetic schemes of the changes of the mixture phase compositions during the treatment of REE sulfates in streams of H_2 are not found in the literature.

The particle morphology and its changes during reactions are of particular importance in heterogeneous reactions. It was shown in [10] that during the interaction between $Ln_2O_2SO_4$ and a hydrogen stream, grains of the Ln_2O_2S crystalline phase are formed from the surface of the precursor particles of the initial material. It is interesting to trace the path of the formation of new phases during the processing of REE sulfate in a hydrogen stream.

The aim of this work was to construct the kinetic schemes of chemical transformations that occur

during treatment with anhydrous REE sulfates $Ln_2(SO_4)_3$ in a stream of hydrogen, and to determine the morphology of the particles in mixtures with different phase compositions.

EXPERIMENTAL

Sulfates of REE were obtained from commercially available oxides of brands LaO-D, PrO-M, NO-M, SmO-D. Weighted amounts of REE oxides were dissolved in 65% nitric acid; the equivalent volume of H_2SO_4 was added, and the resulting suspension was evaporated to dryness at temperatures of 90–100°C. The resulting mixture was treated at 600°C until evolution oxides of nitrogen and sulfur ceased.

The samples were ground to fractions of less than 100 μm. A weighed quantity of 10–11 g (~0.02 moles of anhydrous REE sulfate) was loaded in a quartz beaker, which was placed in a quartz reactor with a feed tube. Hydrogen flowed through the reactor, which was placed in a vertical muffle furnace with a pre-set temperature in the range of 400–1100°C. The temperature in the furnace was maintained with a Thermolux thermoregulator. The total error in measuring the temperature in the reaction zone was ±10 K. The flow rate of hydrogen was 7–8 L/h. The presence of hydrogen sulfide in the reaction products (reaction (I)) was determined from the formation of the precipitate formed by bubbling the outlet gas through a solution of copper sulfate.

At the selected stages of synthesis, the sealed reactor was cooled in air using an air–water mixture. A sample was taken from the inner beaker containing the formed material. X-ray diffraction (XRD) measurements were performed on a DRON-7 diffractometer in CuK_α-radiation (Ni-filter). For sharper reflections in the diffractograms, the samples were treated at 800°C for 10 min in an open reactor filled with argon. The licensed PCPDFW database and PDWin software package were used to identify the diffraction patterns of the samples.

A JEOL JSM-6510 LV scanning electron microscope equipped with an energy dispersive X-ray analyzer was used for X-ray analysis of the particles of the initial REE sulfates and oxysulfides.

RESULTS AND DISCUSSION

Kinetic schemes of the changes in the phase composition of the mixtures while the anhydrous REE sulfates were exposed to an excess hydrogen flow in the temperature range of 400–1100°C were built for the first time. The following chemical reactions were considered:

$$Ln_2(SO_4)_3 + 6H_2 \rightarrow Ln_2O_2SO_4 + 2S + 6H_2O, \quad (I)$$

$$Ln_2O_2SO_4 + 4H_2 \rightarrow Ln_2O_2S + 4H_2O, \quad (II)$$

$$Ln_2O_2SO_4 + H_2 \rightarrow Ln_2O_3 + SO_2 + H_2O, \quad (III)$$

$$S + H_2 \rightarrow H_2S. \quad (IV)$$

Temperatures (°C) of the reaction zone at which the presence of $Ln_2O_2SO_4$ phase (reaction (I)) was recorded via XRD and H_2S was detected in the exhausted gases were found to be 530–535 (La), 460–470 (Pr), 480–490 (Nd), and 490–500 (Sm). The higher temperature of $La_2O_2SO_4$ formation in a mixture was due to lanthanum being a *5d*-element ($4f^05d^16s^2$). There was a trend toward a temperature increase for the products formed in reaction (I) in the series of compounds of 4*f*-elements: Pr ($4f^35d^06s^2$), Nd ($4f^45d^06s^2$), Sm ($4f^65d^06s^2$).

When we used a mixture of REE sulfates subjected only to drying [9], the processing temperatures resulting in the formation of $Ln_2O_2SO_4$ phase fell on average by 20–30 K, but such mixtures could be partially sintered.

Single-phase samples of $Ln_2O_2SO_4$ compounds were obtained at the following temperatures (°C): 540–560 (La), 460–520 (Pr), 470–520 (Nd), and 480–520 (Sm). The required exposure to the hydrogen flow was more than 120 min.

Reaction (I) changed the particle morphology. According to scanning electron microscopy, a mixture of anhydrous REE sulfates was mainly formed by elongated oval-type subgrains in the shape of curved cylinders with diameters of 0.2–0.5 μm and average lengths of 1–5 μm, and by partially flat particles (Fig. 2a). Clumped subgrains formed oval or flat agglomerates with sizes of 5–50 μm. The particles of $La_2O_2SO_4$ phase within each particle had a uniform grain structure without subgrains. The initial subgrains of REE sulfates were combined into single particles of $La_2O_2SO_4$ phases consisting of flake fractals with dimensions of 0.1–0.3 μm (Fig. 2).

The resulting particles of the $Ln_2O_2SO_4$ phase (Fig. 2) had defects that caused blurring of the peaks in the diffraction patterns (Fig. 3). It is possible that such blurring was due to the presence of nanosized flakes in the grain structure [12–14] (Fig. 2b).

In the diffraction patterns of identical samples annealed in an air–argon atmosphere at 800°C for 0.5 h, we see narrow reflections allowing determination of the unit cell parameters of the phases (table, Fig. 3). The field of the $Ln_2O_2SO_4$ single phases is represented in the kinetic schemes by a narrow range of temperatures (Figs. 1a, 1c, 1d).

The interaction between the hydrogen flow and the initial material at 550–570°C led to the formation of REE dioxosulfides Ln_2O_2S (reaction (II)). The reflexes of the Ln_2O_2S phases appear in the diffraction patterns of samples, the intensity of which rose during the process. After 420 min of hydrogen treatment at 550–570°C, the samples remained biphasic: $Ln_2O_2SO_4 + Ln_2O_2S$.

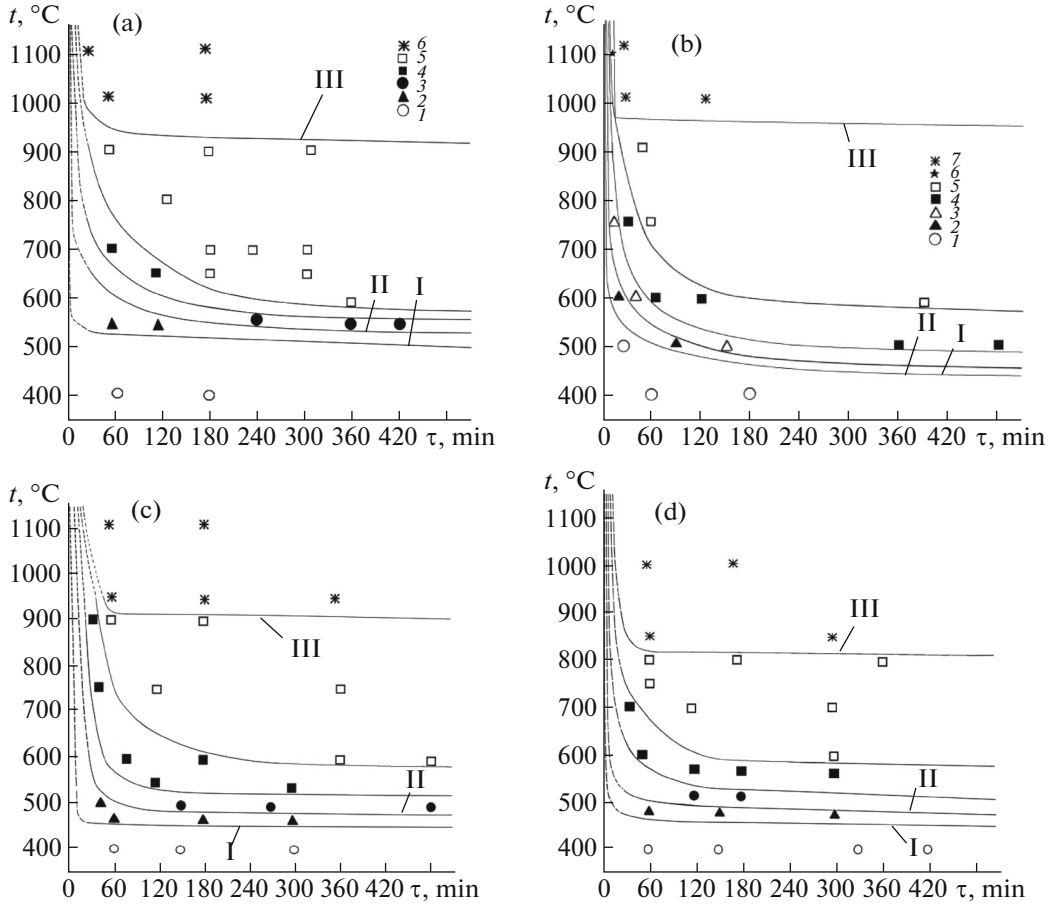

Fig. 1. Kinetic schemes of the changes in the phase composition of materials after exposure to excess H_2 on phases of (a, b) $Ln_2(SO_4)_3$ Ln = La, (c) Nd, and (d) Sm in temperature–time coordinates. Phase composition in systems (a, c, d): (*1*) $Ln_2(SO_4)_3$; (*2*) $Ln_2(SO_4)_3 + Ln_2O_2SO_4$; (*3*) $Ln_2O_2SO_4$; (*4*) $Ln_2O_2SO_4 + Ln_2O_2S$; (*5*) Ln_2O_2S; (*6*) $Ln_2O_2S + Ln_2O_3$. (b) (*1*) $La_2(SO_4)_3$; (*2*) $La_2(SO_4)_3 + La_2O_2SO_4$; (*3*) $La_2(SO_4)_3 + La_2O_2SO_4 + La_2O_2S$; (*4*) $La_2O_2SO_4 + La_2O_2S$; (*5*) La_2O_2S; (*6*) $La_2O_2S + La_2O_3$; (*7*) $La_2O_2SO_4 + La_2O_2S + La_2O_3$.

Single-phase samples of Ln_2O_2S compounds were obtained after 300–350 min of exposure to excessive amounts of hydrogen at 600°C (table, Fig. 1). Increasing the temperature of the reaction zone to 750–900°C reduced the time needed to achieve a single-phase state by a factor of 8–10 and increased the degree of grain crystallinity for the samples of Ln_2O_2S compounds.

The temperature ranges (°C) corresponding to the formation of single-phase samples of Ln_2O_2S fell naturally decreasing in the series of REEs: 580–920 (La), 600–900 (Pr), 600–900 (Nd), and 600–800 (Sm) (Fig. 1).

The values of the processing temperatures of samples for which the phases of Ln_2O_3 (products of reaction (III)) were determined in the material according to XRD fell monotonically from 950 (La) to 850°C (Sm) in the series La–Pr–Nd–Sm. These results indirectly indicate that the thermodynamic stability increases for Ln_2O_3 and decreases for Ln_2O_2S phases [9, 14, 15].

The particles of single-phase Ln_2O_2S samples had a crystalline grain structure. Flat particles 0.3–1 μm thick with plane dimensions of 3–10 μm (Fig. 2c, the ends of the particles) or agglomerates with sizes of 10–70 μm (Fig. 2d) dominate in the mixture. The unit cell parameters of the $Ln_2O_2SO_4$ and Ln_2O_2S compounds correspond to the new data in [2, 9] (table).

In the kinetic schemes, the number of fields of the phase combinations for the REE sulfates' interaction with hydrogen was determined by such factors as temperature and time, as is reflected in the schemes' coordinates; and by the size, shape, and chemical activity of the particles in the material. Two variants of the kinetic schemes are possible; they differ by the combinations of the number of fields and their sequences, determined by the consecutive or parallel course of reactions (I) and (II) throughout the volume of the material.

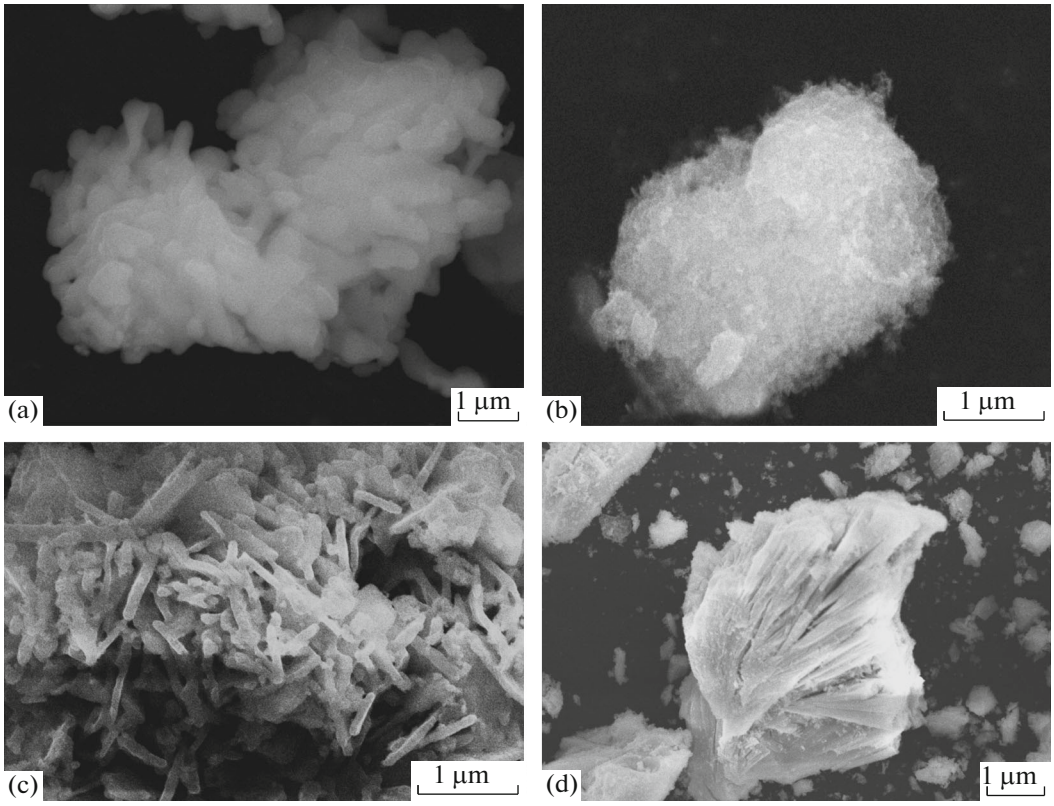

Fig. 2. Images of mixtures of (a) anhydrous lanthanum sulfate, (b) oxolanthanum sulfate, (c) La_2O_2S, (d) Pr_2O_2S.

During the interaction between hydrogen and a uniform mixture of REE sulfates consisting predominantly of particle fractions of 30–5 μm or less, reactions (I) and (II) occur in sequence throughout the volume of the material upon an increase in temperature, according to scanning electron microscopy.

Phase composition of the material during its processing in a hydrogen stream and parameters of the unit cell of the phases, Å

Source sulfate $Ln_2(SO_4)_3$	Temperature and duration of treatment in H_2 stream		
	45 min at 600°C $Ln_2(SO_4)_3$ + $Ln_2O_2SO_4$ (Fig. 1, composition 2)	50 min at 900°C Ln_2O_2S (Fig. 1, composition 5)	120 min at 1050°C Ln_2O_2S + Ln_2O_3 (Fig. 1, composition 6)
$La_2(SO_4)_3$	$La_2(SO_4)_3$ *a* | *b* | *c* 18.39 | 12.5 | 8.77 $La_2O_2SO_4$ 6.91 | 6.91 | 2.15	La_2O_2S (S.G. $P\bar{3}m1$) *a* | *c* 4. 051 | 6. 944	La_2O_2S (S.G. $P\bar{3}m1$) *a* | *c* 4.049 | 6.944 La_2O_3 (S.G. $P6_3/mmc$) 3.962 | 6.166
$Pr_2(SO_4)_3$	$Pr_2(SO_4)_3$ 21.55 | 6.90 | 6.72 $Pr_2O_2SO_4$ 4.29 | 4.20 | 13.25	Pr_2O_2S 3.975 | 6.830	Pr_2O_2S (S.G. $P\bar{3}m1$) 3.974 | 7.100 Pr_6O_{11} (S.G. $Fm3m$)) $a = 5.449$
$Nd_2(SO_4)_3$	$Nd_2(SO_4)_3$ 21.55 | 6.88 | 6.67 $Nd_2O_2SO_4$ 4.24 | 4.10 | 13.30	Nd_2O_2S 3.949 | 6.792	Nd_2O_2S (S.G. $P\bar{3}m1$) 3.945 | 6.788 Nd_2O_3 (S.G. $P6_3/mmc$) 3.968 | 6.302
$Sm_2(SO_4)_3$	$Sm_2(SO_4)_3$ 20.58 | 6.27 | 6.38 $Sm_2O_2SO_4$ 4.30 | 4.08 | 12.69	Sm_2O_2S 3.897 | 6.718	Sm_2O_2S (S.G. $P3m1$) 3.891 | 7.711 Sm_2O_3 (S.G. $P6_3/mmc$) 3.876 | 6.191

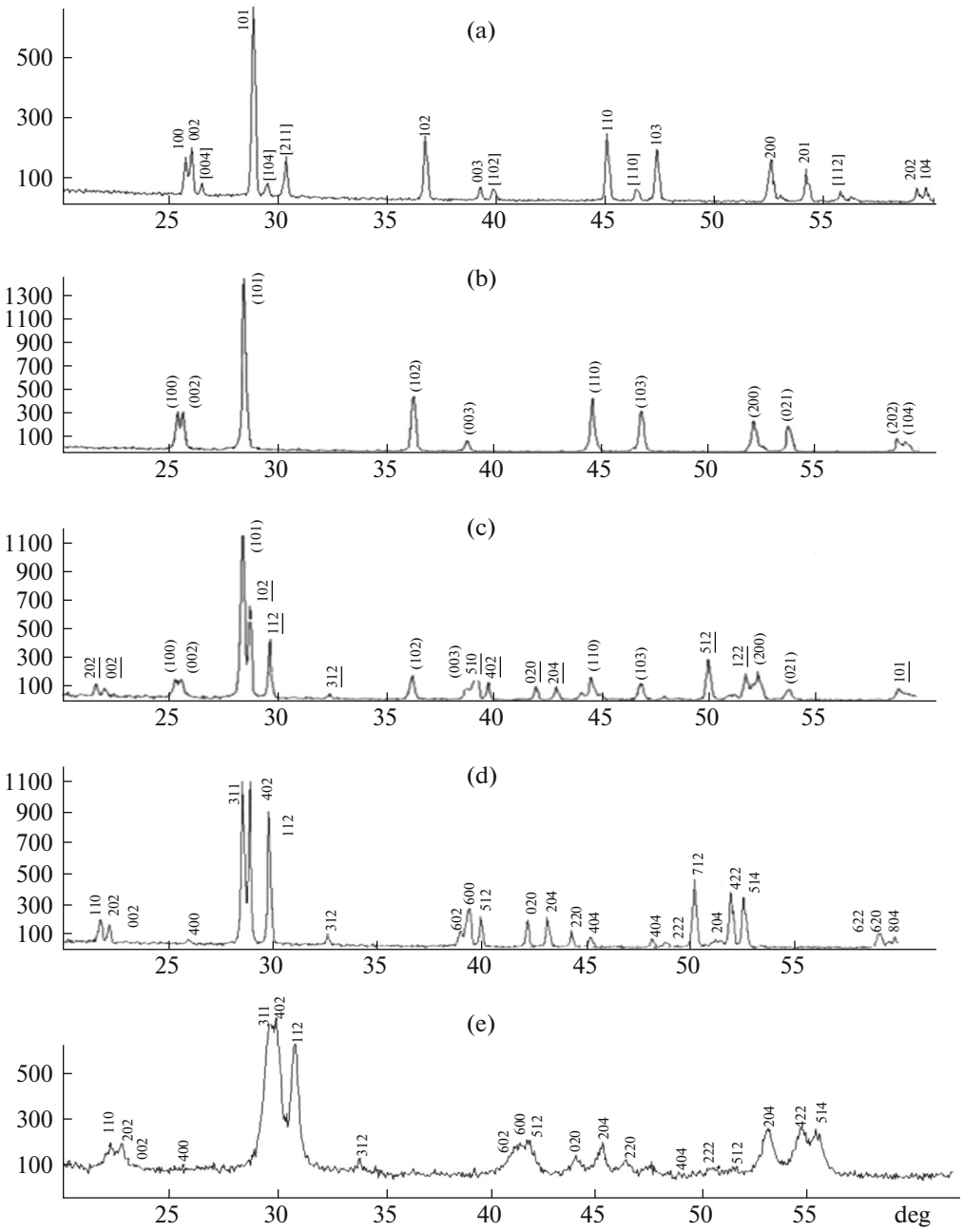

Fig. 3. Diffraction patterns of samples (a) 80 mol % La_2O_2S + 20 mol % La_2O_3; (b) La_2O_2S (a = 0.694 nm, c = 0.405 nm); (c) 80 mol % $La_2O_2SO_4$ + 20 mol % La_2O_2S; (d) neodymium sulfate after 10 h in a stream of hydrogen at 500°C + 2 h at 800°C in air (100 mol $Nd_2O_2SO_4$); (e) neodymium sulfate after 10 h a stream of hydrogen at 500°C (100 mol $Nd_2O_2SO_4$). Notations: $\underline{112}$—$La_2O_2SO_4$; (101)—La_2O_2S.

Under these circumstances, samples of single-phase $Ln_2O_2SO_4$, Ln_2O_2S compounds are formed that are represented in the kinetic schemes and separated by two-phase fields (Fig. 1a).

With nonuniformity of the material and the presence of large crystal agglomerates (up to 100 μm or more), reactions (I) and (II) proceed in parallel, leading to the following arrangement of the fields in the kinetic scheme: $Ln_2(SO_4)_3 \rightarrow Ln_2(SO_4)_3 + Ln_2O_2SO_4 \rightarrow Ln_2(SO_4)_3 + Ln_2O_2SO_4 + Ln_2O_2S \rightarrow Ln_2O_2SO_4 + Ln_2O_2S$ (Fig. 1b). Scheme 1b the one most often observed in experiments [6–10]. One should have specially prepared burden materials for realization of scheme 1a. To meet the conditions of consecutive reactions (I) and (II) at processing times of up to 30 min, the estimated particle size must be less than 10 μm.

The lines delimiting the field of combinations of phases at processing times of 30–420 min were extra-

polated to the area of short-term treatments. The states of the material under these conditions must be considered as hypothetical possibilities. At temperatures above 1000°C, it might be possible to obtain a mixture consisting of all phases included in reaction equations (I)–(III).

CONCLUSIONS

Our kinetic schemes could serve as a basis for determining the conditions needed to obtain single-phase samples of $Ln_2O_2SO_4$, Ln_2O_2S compounds or samples with required phase compositions, e.g., samples of the Ln_2O_2S phase that contain uniformly distributed particles of the Ln_2O_3 phases.

ACKNOWLEDGMENTS

This work was performed with the support of State Contract nos. 2014/228, NIP 996.

REFERENCES

1. Yu. V. Orlovskii, T. T. Basiev, K. K. Pukhov, et al., J. Luminesc. **125**, 201 (2007).
2. Yu. L. Suponitskii, G. M. Kuz'micheva, and A. A. Eliseev, Russ. Chem. Rev. **57**, 209 (1988).
3. A. A. Kirillovich, Extended Abstract of Cand. Sci. (Phys. Math.) Dissertation (Mosc. Eng.-Tech. Inst., Moscow, 1989).
4. O. Ya. Manashirov, D. K. Satarov, V. B. Smirnov, et al., Neorg. Mater. **29**, 1289 (1993).
5. S. A. Osseni, S. Lechevallier, M. Verelst, et al., J. Mater. Chem. **21**, 18365 (2011).
6. E. I. Sal'nikova, P. O. Andreev, and S. M. Antonov, Russ. J. Phys. Chem. A **87**, 1280 (2013).
7. P. O. Andreev, E. I. Sal'nikova, and A. A. Kislitsyn, Russ. J. Phys. Chem. A **87**, 1482 (2013).
8. E. I. Sal'nikova, D. I. Kaliev, and P. O. Andreev, Russ. J. Phys. Chem. A **85**, 2121 (2011).
9. P. O. Andreev, E. I. Sal'nikova, and I. M. Kovenskii, Inorg. Mater. **50**, 1018 (2014).
10. O. V. Andreev, E. I. Sal'nikova, and D. V. Zhuravskii, Vestn. Tyumen. Univ., No. 3, 215 (2010).
11. M. V. Belobeletskaya, N. I. Steblevskaya, and M. A. Medkov, Vestn. DVO RAN, No. **5**, 33 (2013).
12. O. V. Andreev, A. A. Vakulin, and K. V. Kiseleva, *Materials Science* (Tyumen. Gos. Univ., Tyumen', 2013) [in Russian].
13. O. V. Andreev, A. S. Vysokikh, and V. G. Vaulin, Russ. J. Inorg. Chem. **53**, 1320 (2008).
14. O. V. Andreev and O. G. Mikhalkina, Vestn. Omsk. Univ., No. 4, 88 (2012).
15. R. F. Balabaeva, Vestn. Yarosl. Univ., No. 2, 88 (2012).

Translated by A. Pashigreva